A Numerical Simulation of Resonant Extraction

John A. Johnstone
Fermi National Accelerator Lab
October 8, 1993

Introduction

Slow extraction at the Injector is accomplished through excitation of the half-integer resonance. Octupoles distributed on the 0th-harmonic produce the amplitude-dependent tune shift, while two orthogonal families of quadrupoles distributed on the 53rd-harmonic provide the half-integer driving term. One family alone produces the desired phase-space for extraction, while both families are available to correct the intrinsic half-integer stopband of the machine.

An idealized analysis and tracking simulation of the system dynamics was described in MI-0091[1]. The current note reports results obtained from a more realistic simulation of the extraction process. Here, the lattice desprition is refined to include the full complement of magnetic field and alignment errors[2]. Also, the tracking module of the accelerator program MAD[3] is used to propagate particles through the lattice via 2nd-order transfer matrices.

In the following section, correction of the more important errors in the ring is discussed. Subsequently, the slow extraction simulation tracks 1000 particles in this corrected machine and, finally, the results are summarized.

Closed Orbit & Quadrupole Error Corrections

The integrity of the phase space during resonant extraction is most sensitive to closed orbit and quadrupole errors. The circulating beam can be very broad (≈ 60 mm) so large deviations from the design trajectory expose a significant portion of the beam to regions of poor magnetic field quality, resulting in corruption of the phase-space. Quadrupole errors in the ring propagate at twice the tune and contribute an additional (unwanted) half-integer driving term.

[1] J.A. Johnstone, A Simplified Analysis of Resonant Extraction at the Main Injector, MI-91.
[2] F.A. Harfoush, S. Mishra, Systematic & Random Errors for M.I. Tracking, MI-66.
[3] H. Grote, F.C. Iselin, The MAD Program, CERN/SL/90-13(AP).

Of these two error sources the latter is more destructive. The central orbit is corrected irrespective of slow spill considerations, so in the context of the current discussion this is merely a technical detail. Quadrupole errors, on the other hand, are not of particular concern at the normal operating tune of $\nu_x = .425$, but produce major distortions in the horizontal amplitude near the half-integer.

In the slow spill simulation correction of these machine imperfections proceeds as follows: magnetic field and alignment errors, generated by MAD's intrinsic Gaussian random number generator, are assigned to the appropriate lattice elements. Based on the BPM readings trim dipoles correct the central trajectory through the MICADO algorithm. The two 53rd-harmonic quadrupole circuits are then used to measure (and cancel) the intrinsic half-integer stopband.
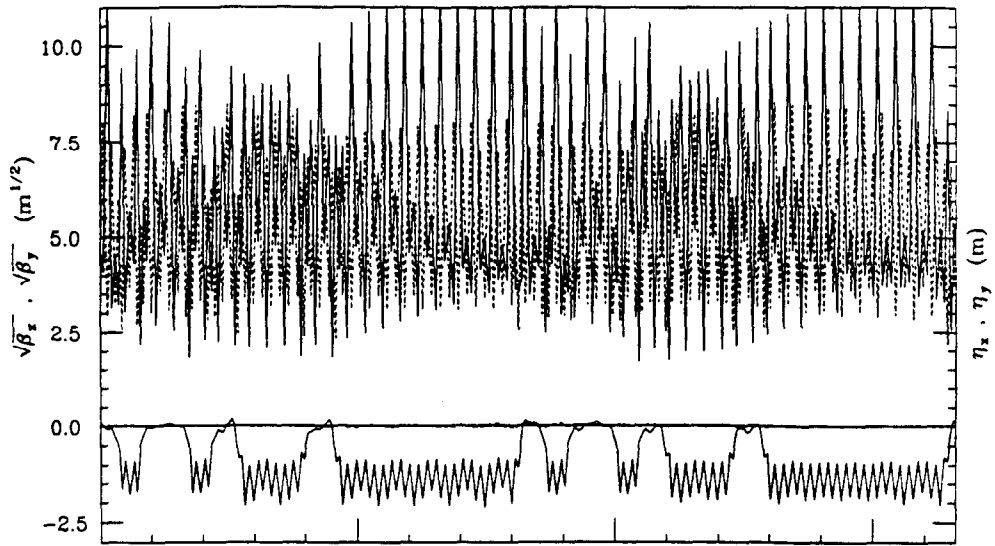
For one particular random generator seed, the BPM readings before correction and the trim strengths required to reduce all readings essentially to zero are summarized in Table 1. The maximum kick of 98 μr is comfortably below the 150 μr available at 120 GeV/c. The corresponding lattice functions are shown in Fig.1 before and after closed orbit correction. Correcting the central trajectory reduces the maximum horizontal amplitude β_x from 144 m to 100 m (compared to the design maximum of 60 m). The large residual variations in β_x are due primarily to quadrupole errors driving the half-integer resonance.

```
------------------------------------------------------------------------
Monitor readings (before correction) for beam line MI18
------------------------------------------------------------------------
Summary:            horizontal                  vertical
total monitors:          104                         104
minimum readings:   -12.354680 mm              -4.435921 mm
minimum positions:   BPMF    [   52]            BPMD    [   27]
maximum readings:    11.408991 mm               5.203012 mm
maximum positions:   BPMF    [   85]            BPMD    [   25]
r.m.s. readings:      6.165719 mm               2.022623 mm
used monitors:           104                         104
------------------------------------------------------------------------


------------------------------------------------------------------------
Corrector strengths (after correction) for beam line MI18
------------------------------------------------------------------------
Summary:            horizontal                  vertical
total correctors:        104                         104
maximum strengths:    0.098061 mrad              0.036175 mrad
maximum positions:   HCORR   [   45]            VCORR   [   23]
r.m.s.  strengths:    0.025707 mrad              0.013643 mrad
used correctors:         104                         104
------------------------------------------------------------------------
```

Table 1: Monitor readings and trim strengths for central trajectory correction.

Qx = .485, Qy = .415: Uncorrected Orbit

Qx = .485, Qy = .415: Corrected Orbit

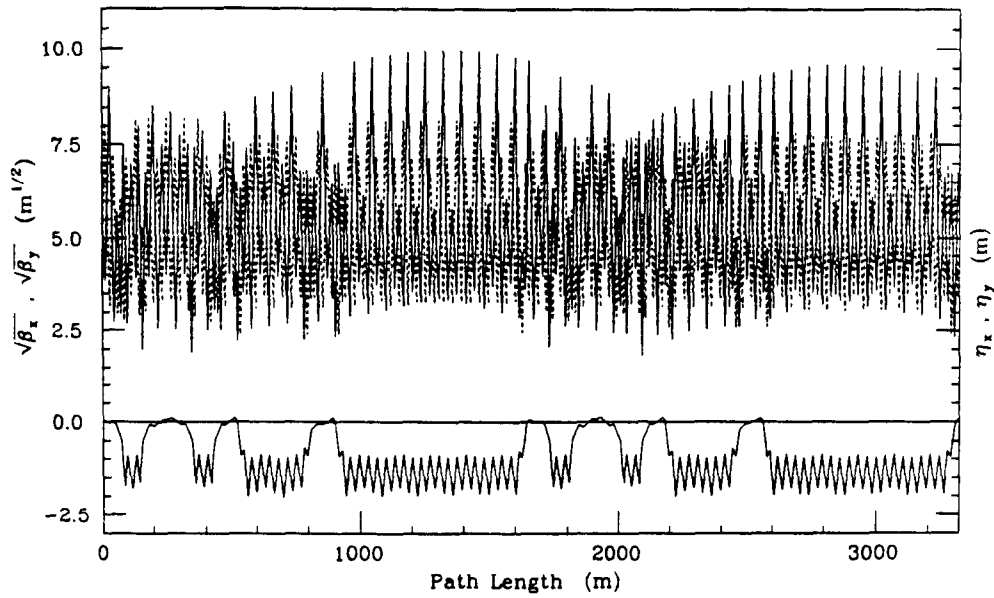Figure 1: Lattice functions before and after central trajectory correction.
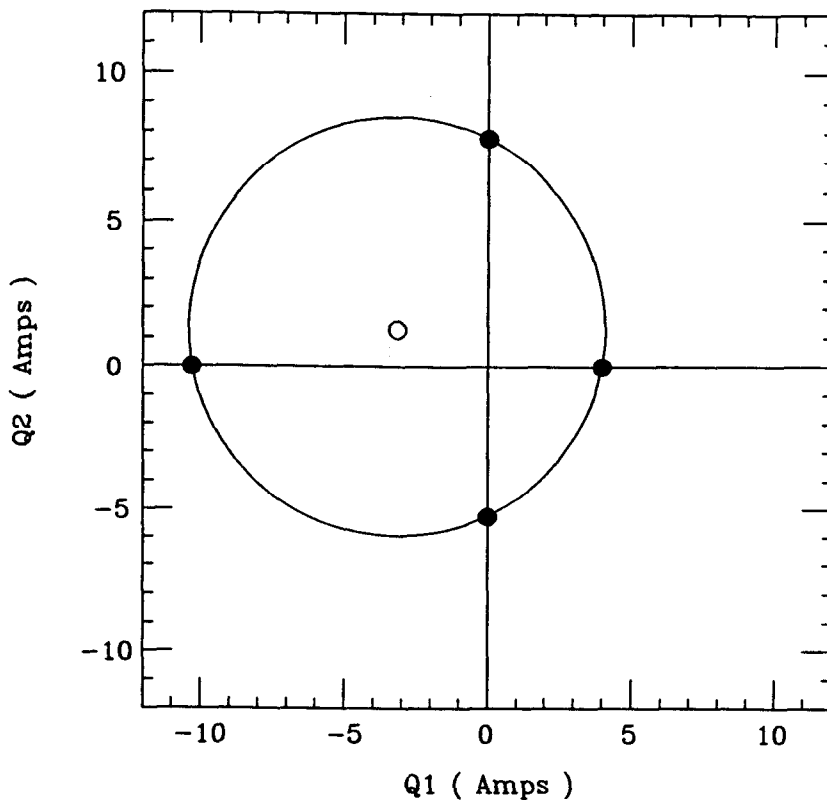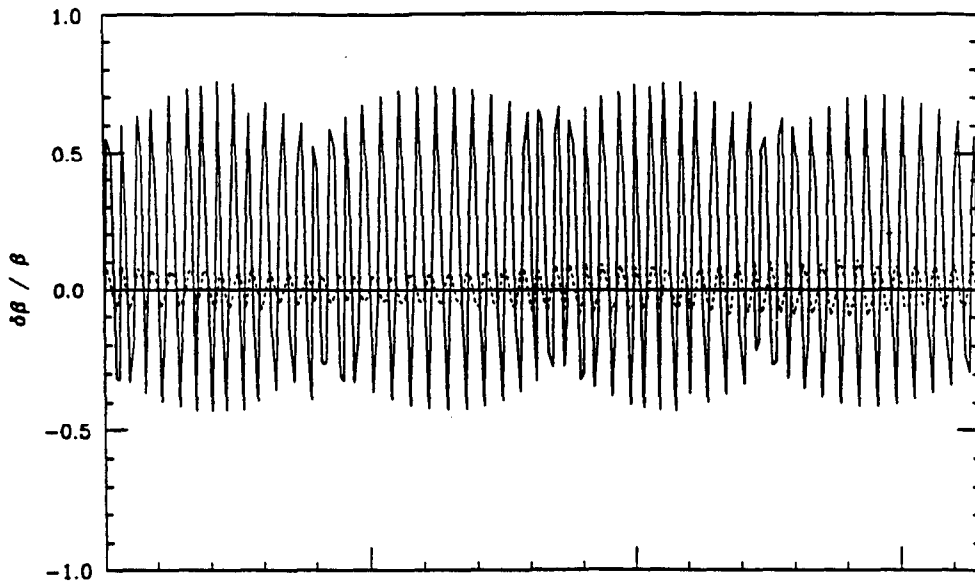
3

Figure 2: Measurement of the natural half-integer stopband.

The technique for quadrupole error compensation is illustrated by Fig.2. Starting from the base tune of $\nu_x = .485$ the 53rd-harmonic quadrupole circuits are ramped independently through both positive and negative values to reach resonance. In the absence of dynamic non-linearities these four points lie on the circumference of a circle. The circle center defines the natural stopband width and phase, and hence the currents Q_1 and Q_2 required to cancel it.

In Fig.3 the variation $\Delta\beta/\beta$ around the ring is shown before and after compensating for the stopband. The improvement is enormous: the maximum $\Delta\beta_x/\beta_x$ deviation is reduced from 76% to only 6%, and the RMS deviation reduced from 41% to 3%. The gain is emphasized by Fig.4 which compares the lattice functions of the corrected machine with the design values.

4

Qx = .485: β Deviation – Corrected Orbit

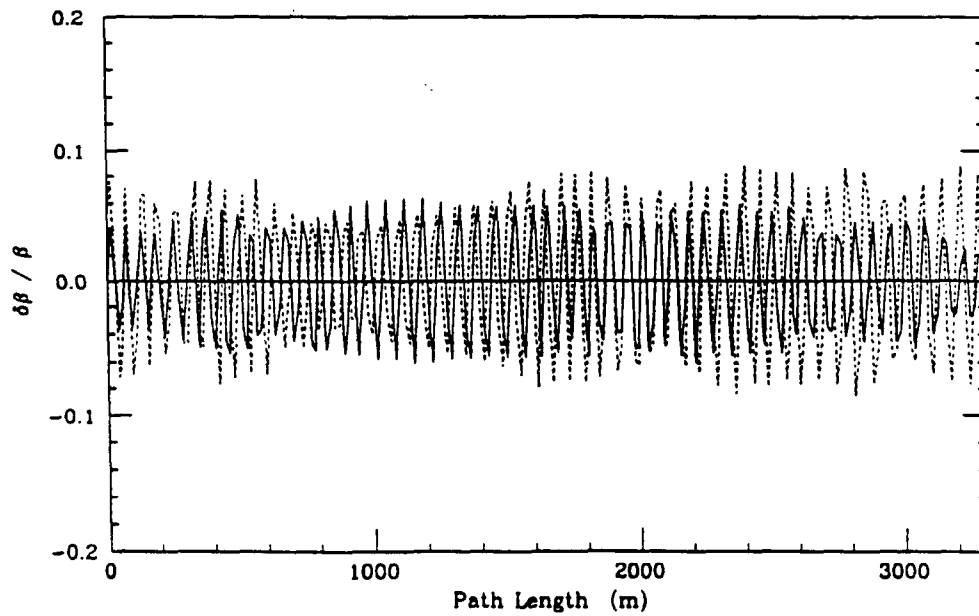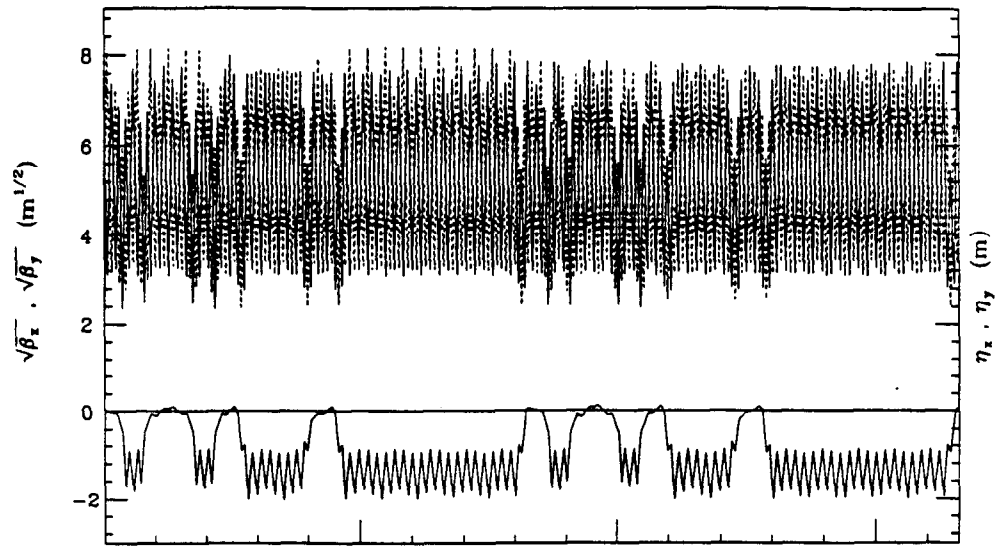**Qx = .485: β Deviation – Corrected Stopband**

Figure 3: $\Delta\beta/\beta$ before and after correcting quadrupole errors.

5

Qx = .485, Qy = .415: Corrected Stopband

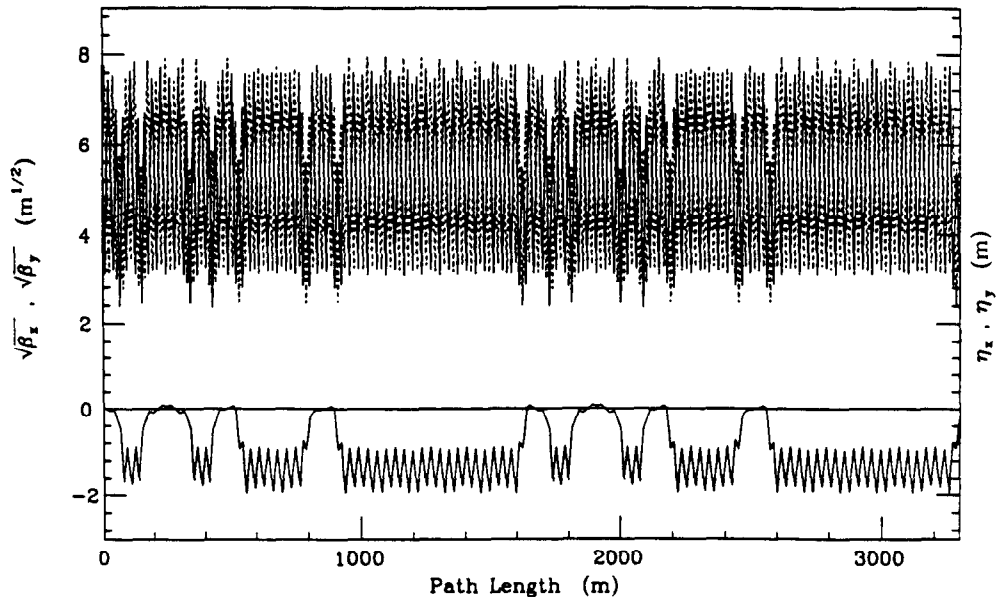Qx = .485, Qy = .415: Design Lattice

Figure 4: Lattice functions after correcting quadrupole errors and design.

6

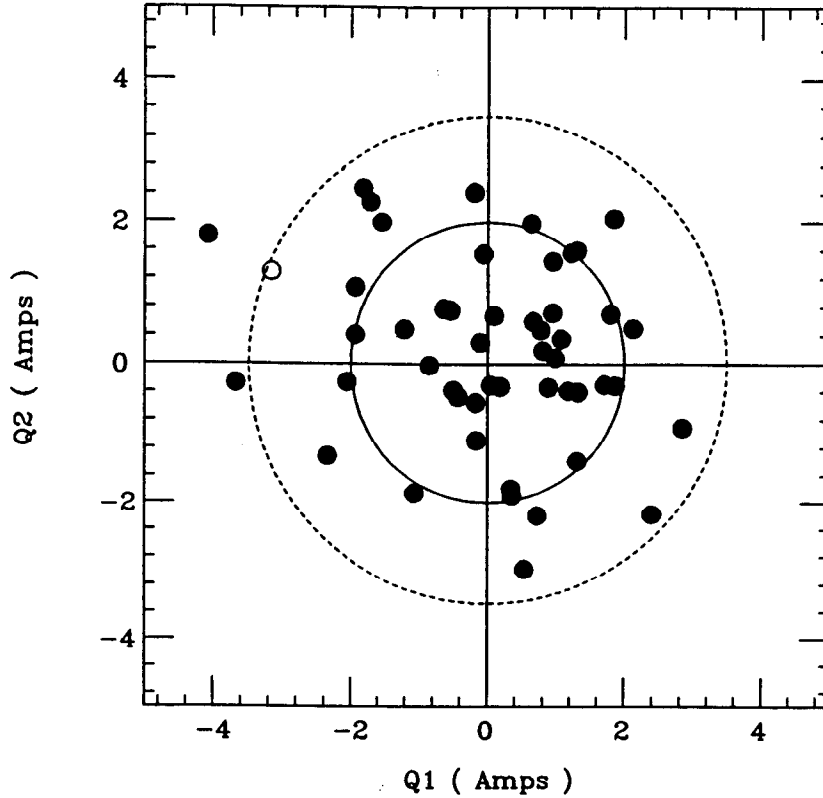Stopband Width & Phase for 50 Random Seeds

Figure 5: Distribution of stopbands from 50 random generator seeds.

The routine just described for correcting orbit and quadrupole errors has been repeated for 50 initial random generator seeds. The resulting distribution of natural stopbands is shown in Fig.5. The magnitudes of quadrupole current $|Q| = (Q_1^2 + Q_2^2)^{1/2}$ necessary to cancel the stopband are well represented by a Gaussian probability density with RMS current $< Q^2 >^{1/2} = 2.0$ Amps. The solid line in Fig.5 corresponds to $|Q| = Q_{RMS}$, and the dashed line is the contour calculated to enclose 95% of all points.

The open circle in Fig.5 at $(Q_1, Q_2) = $ (-3.2,1.3)Amps results from the particular set of machine errors discussed earlier and, lying on the 95% contour, represents in some sense a 'worst-case' scenario. This same machine description is used in the following section for the slow extraction simulation.

7

Simulation of Resonant Extraction

Slow spill takes place from the MI-52 straight section. Three 3.048 m electrostatic septum modules are located immediately upstream of quad #521. The entrance to the first extraction Lambertson is 70^0 in betatron phase downstream from the septa midpoint. The septa wires (of width 0.1 mm) are offset -16 mm from beamline center[4]. Particles that hit the wires during the tracking simulation are considered to be lost, while those that jump across into the extraction channel receive a kick of $325\mu r$. At the Lambertson this kick translates into $\sim$11 mm of separation between extracted and circulating beams.

The initial transverse co-ordinates of 1000 particles are randomly selected from a 30π Gaussian-distributed phase-space. The particles are allowed to circulate unmolested for 100 turns to establish 'steady-state' conditions. During the next 100 turns the harmonic extraction circuits are activated: 0th-harmonic octupoles are ramped to 8.0 Amps, and one family of 53rd-harmonic quadrupoles to 5.5 Amps. At this stage the 30π emittance contour is marginally stable. Extraction occurs over the subsequent 1000 turns. The quadrupoles are further ramped to 7.0 Amps, thereby increasing the width of the half-integer stopband. Gradually all the particles become unstable, stream out along the separatrices, and are extracted. (The short time span used to model the extraction process means that the tracking strictly describes only 'fast' resonant extraction[5]).

The phase-space at the septa entrance and exit is shown in Fig.6. The high density for x $\leq$ -16 mm at the entrance (x $\leq$ -12 mm at the exit) is the phase-space of extracted particles accumulated over the entire cycle. The circulating beam phase-space is a snapshot taken half-way through extraction. During extraction $\sim$2.2% of all particles are lost through collisions with the septa wires.

The corresponding phase-space at the entrance to the Lambertson, and an enlargement of the extracted beam phase-space is shown in Fig.7. The smallest circle in phase-space that encompasses all the extracted particles (as illustrated in Fig.7) corresponds to an emittance $\pi\epsilon = 0.235\pi$ mm-mr, or a normalized value of $\pi\epsilon_N = 30.05\pi$ mm-mr. Interestingly, with the particular choice of octupole strength used in the simulation, extracted beam emittance is equivalent to that of the original circulating beam.

---

[4]note: x $\leq$ 0 is towards the outside of the ring.

[5]'fast' or not, MAD completes tracking in a time somewhere between forever and never.

Septum Entrance
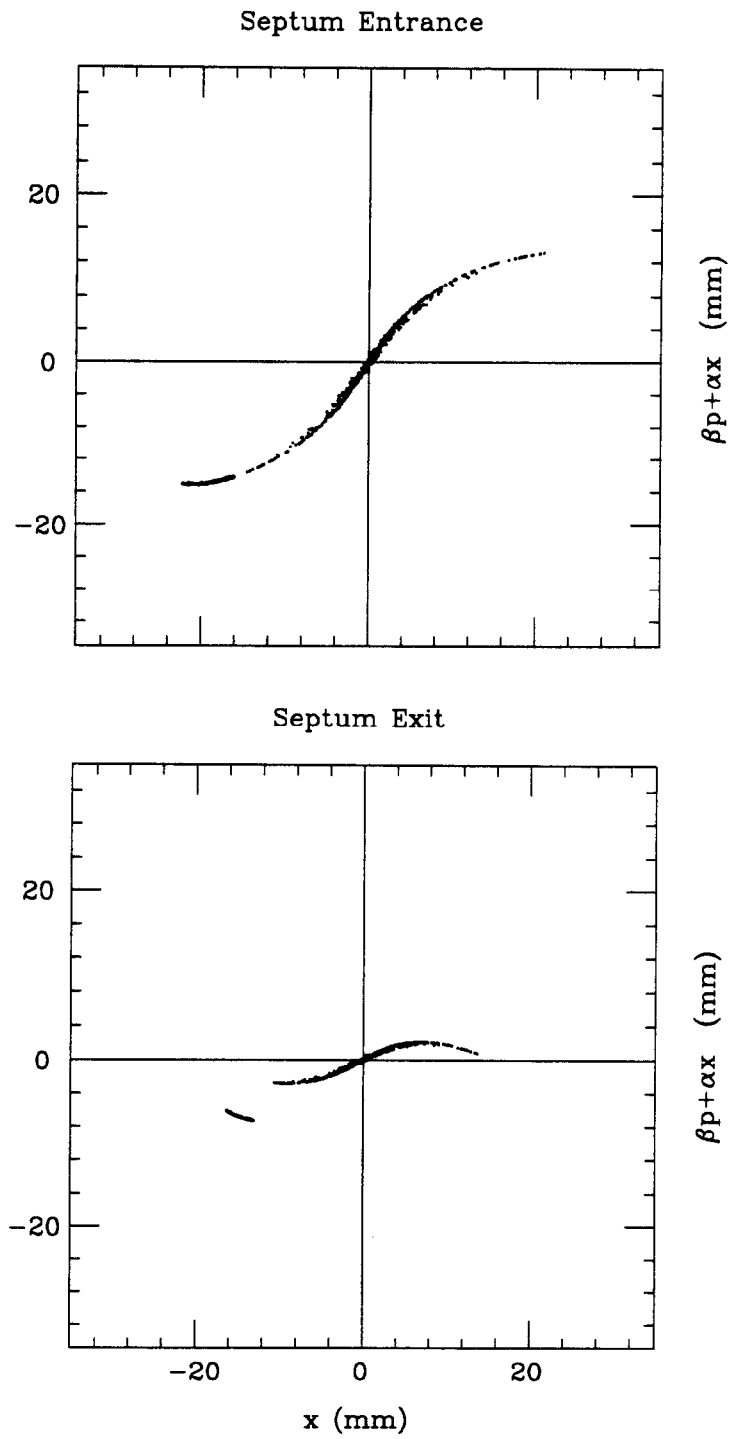

Septum Exit

Figure 6: Phase-space at the entrance and exit of the electrostatic septa.

Lambertson Entrance

$\beta p + \alpha x$ (mm)

x (mm)

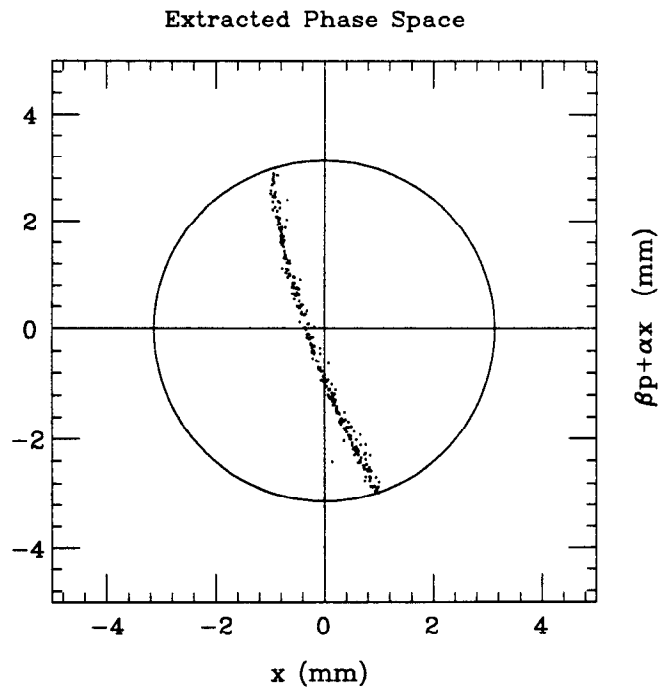Extracted Phase Space

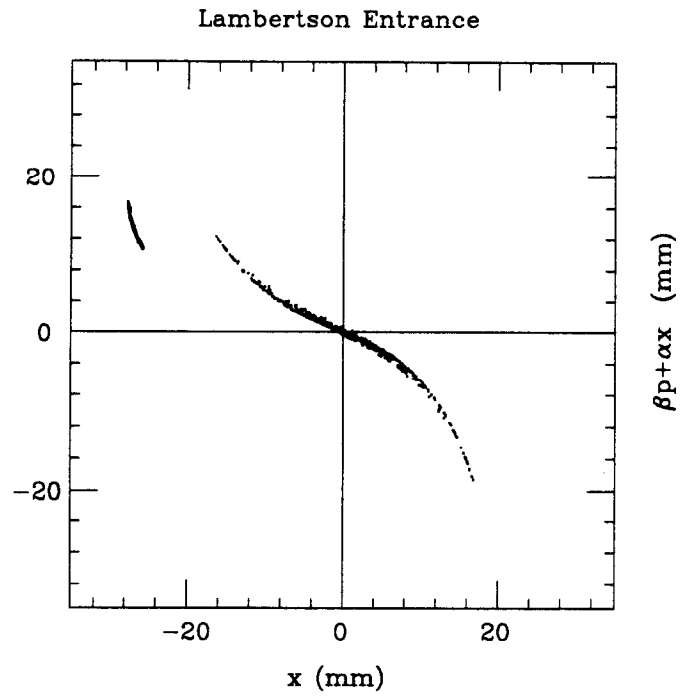$\beta p + \alpha x$ (mm)

x (mm)

Figure 7: Phase-space at the Lambertson and enlargement of extracted beam.

Summary

A realistic description of the Injector lattice, which included all anticipated systematic and random errors, was used in the resonant extraction simulation. Large closed orbit distortions (± 12 mm) were reduced essentially to zero with corrector strengths below their specified limits. The very large β_x variations near the half-integer ($\nu_x = .485$) were eliminated by measuring and cancelling the intrinsic half-integer stopband of the machine with the two families of 53rd-harmonic quads. At this stage the linear lattice functions of the corrected machine differed insignificantly from those of the design lattice.

The simulation tracked 1000 particles through the extraction process. The amplitude-dependent tune-shift was created by 54 0th-harmonic octupoles energized to 8.0 Amps. One family of 8 harmonic quads was ramped to 7.0 Amps, thereby increasing the stopband width, and causing larger amplitude particles to get extracted. The resulting extraction inefficiency of $\sim 2.2\%$, and beam emittance of $\pi \epsilon_N = 30\pi$ mm-mr are acceptable extraction parameters.